


Article

DNA Damage Response Network and Intracellular Redox Status in the Clinical Outcome of Patients with Lung Cancer

Dimitra Mavroei^{1,2}, Anastasia Georganta², Dimitra T. Stefanou³, Christina Papanikolaou¹, Konstantinos N. Syrigos² and Vassilis L. Souliotis^{1,*} 

¹ Institute of Chemical Biology, National Hellenic Research Foundation, 11635 Athens, Greece; dmavro@eie.gr (D.M.); chrpapa@eie.gr (C.P.)

² Third Department of Medicine, Sotiria General Hospital for Chest Diseases, National and Kapodistrian University of Athens, 11527 Athens, Greece; anastgew@med.uoa.gr (A.G.); ksyrigos@med.uoa.gr (K.N.S.)

³ First Department of Internal Medicine, Laikon General Hospital, School of Medicine, National and Kapodistrian University of Athens, 11527 Athens, Greece; dimitroulastef@hotmail.com

* Correspondence: vls@eie.gr

Simple Summary: DNA damage response (DDR) is a multi-factor network that is responsible for the removal of DNA lesions, thus enabling cells to function normally. An imbalance between the generation of reactive oxygen species and their removal by defense mechanisms is known as oxidative stress. Previous studies demonstrated that deregulation of the DDR network and redox imbalance are implicated in the onset and progression of several diseases, including cancer, as well as in the outcome of chemotherapy. In this study, we found that DDR-associated parameters and the intracellular redox status display significant differences among patients with lung cancer at baseline and correlate with the clinical responses to subsequent platinum-based therapy. The exploitation of these results might lead to the identification of new therapeutic targets, the design of effective and sensitive biomarkers, and the development of new therapeutic regimens for the treatment of this devastating malignancy.



Citation: Mavroei, D.; Georganta, A.; Stefanou, D.T.; Papanikolaou, C.; Syrigos, K.N.; Souliotis, V.L. DNA Damage Response Network and Intracellular Redox Status in the Clinical Outcome of Patients with Lung Cancer. *Cancers* **2024**, *16*, 4218. <https://doi.org/10.3390/cancers16244218>

Academic Editors: Arrigo De Benedetti, Mariarita de Felice and Mariarosaria de Falco

Received: 25 November 2024
Revised: 13 December 2024
Accepted: 17 December 2024
Published: 18 December 2024



Copyright: © 2024 by the authors. Licensee MDPI, Basel, Switzerland. This article is an open access article distributed under the terms and conditions of the Creative Commons Attribution (CC BY) license (<https://creativecommons.org/licenses/by/4.0/>).

Abstract: Background/Objectives: DNA damage response (DDR) is a network of molecular pathways associated with the pathogenesis and progression of several diseases, as well as the outcome of chemotherapy. Moreover, the intracellular redox status is essential for maintaining cell viability and controlling cellular signaling. Herein, we analyzed DDR signals and redox status in peripheral blood mononuclear cells (PBMCs) from patients with lung cancer with different response rates to platinum-based chemotherapy. **Methods:** Several DDR-associated signals and redox status, expressed as the GSH/GSSG ratio, were measured in two lung cancer cell lines (A549, H1299), two normal fibroblast cell lines (WS1, 1BR3hT), and PBMCs from 20 healthy controls and 32 patients with lung cancer at baseline (17 responders and 15 non-responders to subsequent platinum-based chemotherapy). **Results:** Higher levels of endogenous/baseline DNA damage, decreased GSH/GSSG ratios, and augmented apurinic/aprimidinic sites, as well as lower nucleotide excision repair (NER) and increased interstrand cross-links (ICLs) repair efficiencies, were observed in lung cancer cell lines compared with normal ones (all $p < 0.05$). Moreover, PBMCs from patients with lung cancer showed reduced GSH/GSSG ratios, augmented apurinic/aprimidinic sites, decreased NER and ICL repair capacities, and lower apoptosis rates, compared with healthy controls (all $p < 0.001$). Interestingly, PBMCs from patients who are responders are characterized by reduced GSH/GSSG ratios, augmented apurinic/aprimidinic sites, decreased NER and ICL repair capacities, and higher apoptosis rates compared with patients who are non-responders (all $p < 0.01$). **Conclusions:** Together, DDR-associated parameters and redox status measured in PBMCs from patients with lung cancer at baseline are associated with the therapeutic benefit of platinum-based chemotherapy.

Keywords: DNA damage response (DDR); lung cancer; PBMCs; platinum-based chemotherapy; clinical response; redox status; oxidative stress; apurinic/aprimidinic (AP) sites; nucleotide excision repair (NER); interstrand cross-link repair (ICL/R)

1. Introduction

Lung cancer remains one of the most-diagnosed malignant diseases over decades, characterized by high mortality rates, with over 2 million cases per year rising worldwide [1]. Based on the histology of the cancer cells, lung cancer can be categorized into two types: small cell lung cancer (SCLC), which comprises about 15% of lung cancers, and non-small cell lung cancer (NSCLC), which accounts for 85% of all cases and can be further subdivided into three histological types: adenocarcinoma, large cell carcinoma, and squamous cell carcinoma [2]. Despite considerable progress in understanding, diagnosing, and treating the disease, further advances seem obligatory. One major challenge appears to be the identification of accurate predictive biomarkers that can be utilized in the clinic to improve treatment design [3].

Lung cancer has early been related to cigarette smoking, and many carcinogenic compounds have been identified in tobacco ever since [4]. These substances induce DNA damage, contributing to genomic instability associated with the high mutational burden of lung cancer cells. Nevertheless, a significant percentage of patients who develop lung cancer have not ever used tobacco, implying further DNA-damaging factors, such as environmental pollution, radiation, exposure to industrial hazardous agents, etc., pose as risk factors, interplaying with genetic predisposition [5,6].

The human genome is constantly exposed to multiple exogenous (genotoxic chemicals, UV light, ionizing radiation, etc.) and endogenous DNA-damaging factors (e.g., oxidation, alkylation, hydrolysis, and mismatch of DNA bases) [7–9]. Genotoxic stress may also emerge from several cellular processes, such as replication and transcription [10,11]. Specifically, the generation and response to reactive oxygen species (ROS) remain among the most well-studied genotoxic mechanisms, as cancer cells are frequently characterized by impaired regulation of ROS. Several pathways are involved in ROS regulation, as their function is critical for cell signaling and metabolism. Disrupted ROS levels lead to pathological outcomes and disease development [12,13], while redox status has been highlighted as critical for both cancer progression and chemotherapy response [14]. Particularly in lung cancer, evidence suggests that oxidative stress is critical for the onset and progression of the disease, as lungs are more susceptible due to their exposure to oxygen and blood circulation [15]. Moreover, ROS are capable of directly inducing DNA lesions, including oxidized purines and pyrimidines, single-strand breaks (SSBs), double-strand breaks (DSBs), and abasic (AP; apurinic/aprimidinic) sites [16–18]. Specifically, AP-sites are common DNA lesions that may occur both spontaneously, due to oxidative stress, and as intermediates of DNA repair pathways, such as base excision repair (BER) [19]. Repair of AP-sites includes their cleavage and SSB formation that may result in DSBs during DNA replication. As such, AP-sites levels have been suggested as a possible biomarker for oxidative stress and BER capacity, while it has been proposed that it could even predict survival in patients with resected NSCLC [19]. Moreover, a key factor of BER, the apurinic/aprimidinic endonuclease 1 (APE1), has been underlined as a therapeutic target in NSCLC, as its inhibition resulted in excessive DNA damage and augmented tumor cell death *in vitro* and *in vivo* [20].

Interestingly, genotoxic drugs like platinum-based compounds have been reported to induce oxidative stress-related cytotoxic effects, either by directly generating ROS or by blocking the antioxidant system [21–23]. As a result, redox status appears to be crucial for response to chemotherapy-based treatment [14,24–26]. Glutathione, a key antioxidant factor, has been found to react with cisplatin and regulate resistance to this drug [26–30]. GSH, the reduced form of glutathione, binds and deactivates cisplatin molecules, thus preventing them from reaching the DNA and forming adducts [28,29]. In parallel, GSH reacts with the cisplatin-induced ROS, interfering with ROS-mediated cytotoxicity [29]. In particular, cisplatin cytotoxicity depends on the glutathione levels and the expression of the nuclear factor erythroid 2-related factor 2 (NRF2), which controls the transcription of glutathione components in lung cancer [29] and other tumor cells [31].

To confront the above challenges and ensure genomic stability, cells have developed a complex system of molecules and pathways, commonly known as the DNA damage response (DDR) network, including sensors of the lesion sites, cell cycle kinases, signaling cascades and effector proteins that maintain genomic integrity [32,33]. Disruption of the function of DDR network contributes to genomic instability and is involved in tumorigenesis. Furthermore, recent data have shown that DDR strongly impacts the immune system suggesting crucial therapeutic implications [34,35]. Specifically, defects in repair mechanisms may lead to the accumulation of cytosolic DNA resulting in stimulation of innate immune response and/or genomic mutations. These effects increase tumor mutational burden and levels of MHC-presented neoantigens, thus potentiating anti-tumor immune response [36–38].

Lung cancer is currently commonly treated with chemotherapy, molecular-targeted therapy, immunotherapy, radiation therapy and surgery [1,2]. The standard of care for most advanced NSCLC-patients includes platinum-based chemotherapy [39], thanks to its cytotoxicity. These drugs function by inducing the formation of DNA monoadducts that are almost exclusively repaired by nucleotide excision repair (NER), and interstrand cross-links (ICLs), which are repaired by NER, translesion synthesis, Fanconi anemia pathway, homologous recombination (HR), and nonhomologous end-joining (NHEJ) [18].

In this study, we tested the hypothesis that redox status and DDR-related parameters of patients with lung cancer at baseline correlate with therapeutic benefit from subsequent platinum-based treatment. Towards this, we evaluated GSH/GSSG ratio (a reliable estimation of cellular redox status), apurinic/aprimidinic sites, and several DDR parameters, including the endogenous/baseline DNA damage, the efficiencies of critical DNA repair mechanisms and the apoptosis rates in normal and lung cancer cell lines, as well as in peripheral blood mononuclear cells (PBMCs) from healthy controls and patients with lung cancer at baseline.

2. Materials and Methods

2.1. Patients

A total of 32 patients with lung cancer were included in this study: seventeen ($n = 17$) patients with partial response to therapy (PR; 3 females/14 males; median age, 66 years; range, 49–82), five ($n = 5$) with stable disease (SD; 2 females/3 males; median age, 68 years; range, 65–76), and ten ($n = 10$) with progressive disease (PD; 3 females/7 males; median age, 68.5 years; range, 62–81) (Table 1). Twenty ($n = 20$) healthy individuals were also included as controls (HC; 8 females/12 males; median age 61.4 years; range, 41–82). PBMCs were isolated from freshly drawn peripheral blood and purified using the standard Ficoll gradient centrifugation. Briefly, 10 mL of whole blood were diluted 1:1 in RPMI-1640 medium, carefully layered over 15 mL of Ficoll reagent (Ficoll-Paque PLUS, Sigma-Aldrich, St. Louis, MI, USA, #GE17-1440-03), and centrifuged at $400\times g$ for 20 min at $20\text{ }^{\circ}\text{C}$, without brake or acceleration. After centrifugation, the semi-white layer containing PBMCs was collected using a syringe. The collected cells were transferred to 10 mL of RPMI-1640 medium and washed twice via centrifugation at $400\times g$ for 20 min at $20\text{ }^{\circ}\text{C}$, this time with normal brake and acceleration. Cells were resuspended in freezing medium (90% fetal bovine serum and 10% dimethyl sulfoxide) and stored at $-80\text{ }^{\circ}\text{C}$ until further processing. The study was approved by the Institutional Review Board of Soteria Hospital (No. 15627/11.6.2020 and No. 25950/10.10.2022), and all subjects provided informed consent. The study was conducted according to the Declaration of Helsinki.

2.2. Cell Lines

Human 1BR3hT cells (immortalized normal skin fibroblasts) and H1299 cells (epithelial-like non-small-cell lung carcinoma) were maintained in Dulbecco's modified Eagle's medium (DMEM), 10% fetal bovine serum (FBS), and 1% penicillin/streptomycin (Pen/Strep). Human A549 cells (non-small-cell lung carcinoma) were maintained in DMEM/Ham's F12 (1:1)

medium, 10% FBS, and 1% Pen/Strep. Human WS1 cells (normal skin fibroblasts) were maintained in DMEM, 1% non-essential amino acids, 10% FBS, and 1% Pen/Strep.

Table 1. Patients and disease characteristics.

Patients (N = 32)			
Characteristic	N	Years	% of Total
Sex			
Male	24	-	75
Female	8	-	25
Age			
Median	-	67.5	-
Range	-	49–82	-
Histology			
Squamous	10	-	31.3
Non-squamous	17	-	53.1
Small cell	5	-	15.6
Stage			
I–II/LD	4	-	12.5
III	7	-	21.9
IV	21	-	65.6
Smoking			
Never	3	-	9.3
Current	3	-	9.3
Former	24	-	75
PD-L1 expression			
<1%	7	-	21.9
1–50%	7	-	21.9
>50%	7	-	21.9
Therapy			
Chemotherapy	10	-	31.3
Chemotherapy–radiotherapy combination	8	-	25
Chemotherapy–immunotherapy combination	12	-	37.5
Chemotherapy–immunotherapy–radiotherapy combination	2	-	6.2
Cycles of platinum therapy			
<4	5	-	15.6
4–5	23	-	71.9
6	4	-	12.5
Response			
PR	17	-	53.1
SD	5	-	15.6
PD	10	-	31.3

2.3. Measurement of Nucleotide Excision Repair (NER)—Alkaline Comet Assay

DNA damage was assessed using the alkaline comet assay. Cells suspended in phosphate-buffered saline (PBS; pH 7.4) were mixed with 1% low-melting-point agarose and loaded onto glass slides. The slides were allowed to solidify at 4 °C for 30 min, incubated in an alkaline lysis buffer (2.5 M NaCl, 0.1 M EDTA, 0.01 M Tris; pH 10, 1% Triton X-100) for 2 h at 4 °C, and electrophoresed at 25 V, 225 mA for 30 min. The slides were stained with SYBR™ Gold nucleic acid gel stain (Thermo Fisher Scientific, Waltham, MA, USA, #S11494) and imaged under UV light using a 10× microscopy lens. Olive tail moment (OTM) was analyzed using ImageJ Analysis/OpenComet v1.3.1 (<https://cometbio.org/>). For each sample, 2 gels were scored, and the average OTM value of 150 cells was calculated.

2.4. Measurement of Gene-Specific Repair of the Interstrand Cross-Links

Cell lines or PBMCs were treated with cisplatin (25 µg/mL and 5 µg/mL, respectively) for 3 h at 37 °C in the appropriate culture medium, incubated in drug-free medium for 0–24 h at 37 °C, harvested, and stored in freezing medium at –80 °C. The gene-specific repair of the ICLs was measured using Southern blot analysis, as described previously [40]. For the analysis of N-ras alkylation, after isolation, genomic DNA was digested using the restriction enzyme EcoRI, and DNA samples were denatured prior to gel electrophoresis. That is, DNA was incubated at 37 °C for 15 min in 50 mM NaOH, denaturation was stopped on ice, and DNA samples were mixed with sample loading buffer (final concentration: 0.2% Ficoll, 0.1 mM EDTA, 0.01% bromocresol green). Electrophoresis was performed for 16 h at 30 V in 0.6% agarose gel, using buffer containing 40 mM Tris-acetate and 2 mM EDTA. Hybridizations were performed as previously described [41]. The percentage cross-linking, which is the density of the cross-linked DNA band as a fraction of both single-stranded and cross-linked band densities, was used to calculate the frequency of ICLs. The average number of ICLs per restriction fragment examined was calculated using the formula of the Poisson distribution: (cross-links/fragment) = $-\log_e(\text{fraction of fragment free of cross-links})$.

2.5. GSH/GSSG Ratio and Abasic Sites

The GSH/GSSG ratio was determined using a luminescence-based assay that measures total glutathione (GSH+GSSG), oxidized glutathione (GSSG), and the GSH/GSSG ratio, following the manufacturer's instructions (GSH/GSSG-Glo Assay, Promega, Madison, WI, USA, #V6612). Abasic sites were analyzed with the OxiSelect Oxidative DNA Damage Quantitation Kit (Cell Biolabs, San Diego, CA, USA; #STA-324), also in accordance with the manufacturer's protocol.

2.6. Apoptosis Rates

PBMCs were exposed to varying doses of cisplatin (0–150 µg/mL) for 3 h at 37 °C in complete RPMI-1640 medium, followed by a 24 h incubation in cisplatin-free medium. Apoptosis rates were measured using the Cell Death Detection ELISA PLUS kit (Roche Diagnostics Corp., #11.774.425.001, Mannheim, Germany) according to the manufacturer's instructions.

2.7. Western Blot Analysis

Cell lysates were prepared using the RIPA Lysis Buffer System (Santa Cruz Biotechnology, Dallas, TX, USA, #sc-24948). Protein electrophoresis was carried out on 4–20% FastGene PAGE Gels (Nippon Genetics, Tokyo, Japan, #PG-S420) with MOPS buffer (Nippon Genetics, #PG-MOPS10). Proteins were transferred to nitrocellulose membranes (GE Healthcare, Chicago, IL, USA, Amersham Protran 0.45 µm, #10600002) and incubated overnight at 4 °C with primary antibodies (Cell Signaling Technology, Danvers, MA, USA; γH2AX, #80312; β-tubulin, #15115L; β-actin, #3700). Membranes were incubated with horseradish peroxidase (HRP)-conjugated secondary antibodies (Cell Signaling Technology; anti-mouse IgG: HRP, #7076S; anti-rabbit IgG: HRP, #7074S), the antibody complexes were visualized using the Pierce™ ECL Western Blotting Substrate (Thermo Scientific, #32106) and imaged using the BioRad Gel Doc XR Imaging System.

2.8. Statistical Analysis

An unpaired *t* test with Welch's correction was applied for *p*-value determination. The results were of statistical significance when *p* < 0.05. All statistical analyses and graph design were carried out with GraphPad Prism 8.0.1. The mean ± SD was used to present the data.

3. Results

3.1. DDR-Associated Parameters in Lung Cancer Cell Lines

DDR-related signals were analyzed in two lung cancer cell lines (A549, H1299) and two normal fibroblast cell lines (WS1, 1BR3hT). For all parameters examined, similar results were obtained for the cell lines of each group. First, the endogenous/baseline DNA damage was evaluated using alkaline comet assay, which measures SSBs and/or DSBs. As seen in Figure 1A, the endogenous/baseline DNA damage was found to be significantly higher in lung cancer cell lines than in normal ones ($p < 0.001$), showing accumulation of DNA lesions in malignant cells when there is no known exogenous genotoxic attack. To further investigate the formation of the endogenous/baseline DNA damage, we measured intracellular factors that lead to the formation of SSBs and DSBs, such as redox dysregulation and AP-sites. Interestingly, the GSH/GSSG ratio was found to be decreased, while AP-sites were augmented in cancer cells compared with the normal ones (all $p < 0.001$; Figure 1B,C).

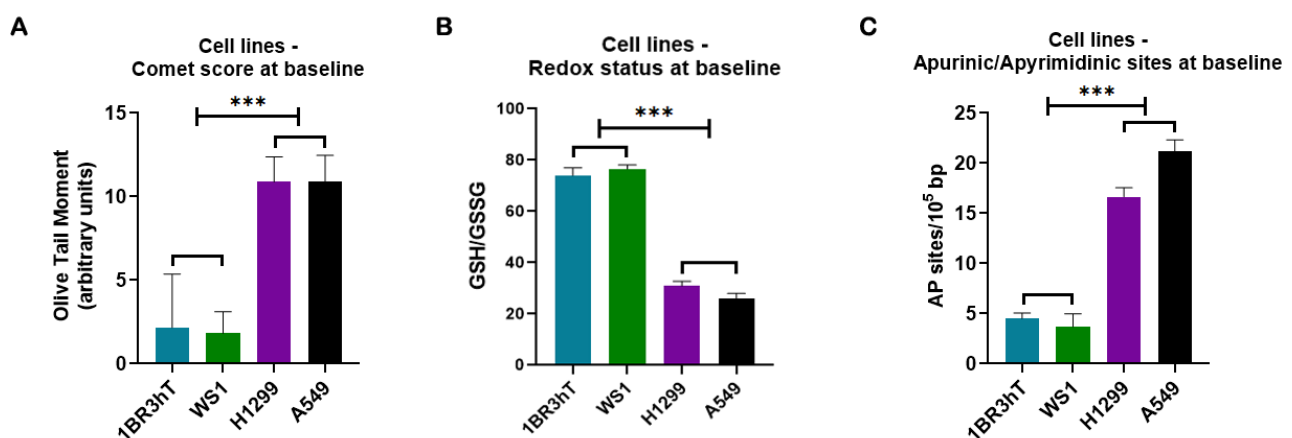


Figure 1. DDR-associated parameters in cell lines at baseline. (A) Bar charts showing the endogenous/baseline DNA damage in normal and lung cancer cell lines measured by comet assay. (B) Redox status expressed by the GSH/GSSG ratio at untreated cell lines. (C) Baseline AP-site levels for all cell lines. Error bars represent SD; *** $p < 0.001$. The experiments shown were based on a minimum of three independent repeats.

Then, the efficiency of NER was evaluated. That is, all cell lines were irradiated with 100 J/m^2 UVC, which induces cyclobutane pyrimidine dimers (CPDs) and 6–4 photoproducts (6-4PPs), DNA lesions that are repaired by the NER pathway [42], and the DNA damage was measured using an alkaline comet assay (Figure 2A). Significant differences in the efficiencies of NER were found between malignant and normal cell lines. Indeed, lung cancer cell lines showed reduced NER efficiency compared with normal cells (Figure 2B), resulting in higher UVC-induced DNA damage accumulation in malignant cells, expressed as the area under the curve (AUC) for DNA damage during the whole experiment (0–6 h) ($p < 0.001$; Figure 2C). Moreover, in both lung cancer and normal cell lines, we found that UVC irradiation reduced the GSH/GSSG ratio and increased AP-sites ($p < 0.05$; Figure 2D,E). Although kinetic patterns of UVC-induced AP-sites showed no significant differences between lung cancer and normal cells (Figure 2E), augmented accumulation of AP-sites was found in the lung cancer cell lines ($p < 0.001$; Figure 2F), due to increased levels of endogenous/baseline AP-sites in these cells. Together, these data suggest that the increased endogenous/baseline levels of DNA damage found in malignant cells may result, at least partly, from disruption of redox homeostasis and the subsequent formation of AP-sites.

To study the efficiency of the ICL repair, cell lines were treated with $25 \mu\text{g/mL}$ cisplatin for 3 h, and the kinetics of ICL repair was followed for up to 24 h after treatment. Significant

differences in the cisplatin-induced ICL burden were found between malignant and normal cell lines, with lung cancer cells showing slightly higher ICL repair capacity ($p < 0.05$; Figure 3A). In addition, in both lung cancer and normal cell lines, cisplatin treatment resulted in a reduction of the GSH/GSSG ratio (Figure 3B) and higher levels of AP-sites (Figure 3C); maximal effect on both factors analyzed was observed at the end of the 3 h cisplatin treatment (time point, T0). Importantly, significant differences were observed in the GSH/GSSG ratio and AP-sites kinetic patterns after cisplatin treatment between lung cancer and normal cells, with the malignant cells returning to baseline levels much faster than normal cells. Moreover, robustly higher total amounts of AP-sites expressed as AUC were found in malignant than in normal cell lines (Figure 3D). Next, the cisplatin-induced phosphorylation of H2AX at the serine residue 139, as a marker of DSBs, was also evaluated. In all cell lines analyzed, maximal levels of γ H2AX were observed at the 24 h time point (Figure 3E).

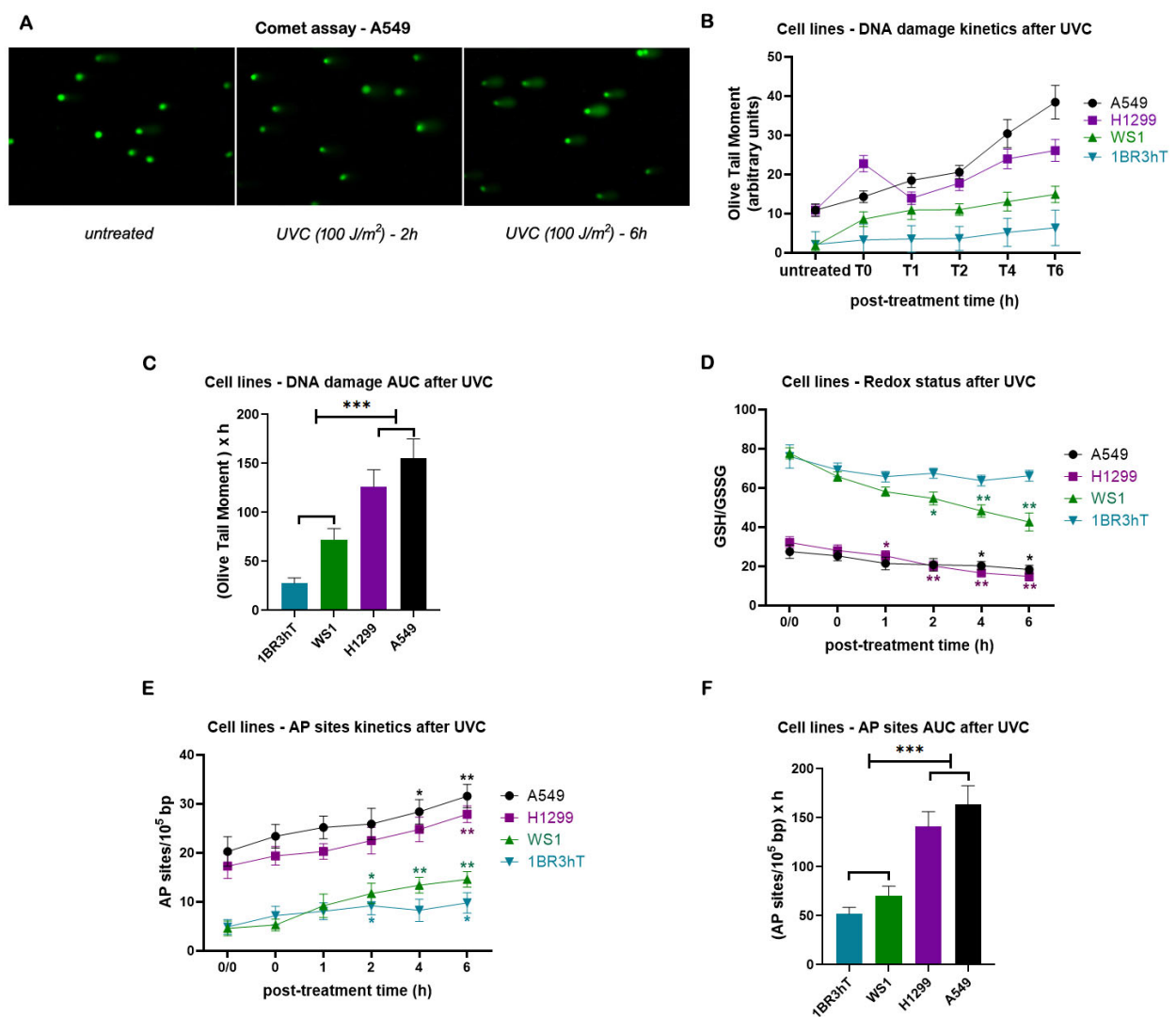


Figure 2. DNA damage response signals in cell lines after UVC irradiation. (A) Alkaline comet assay images of A549 lung cancer cell line at baseline and at different time points after UVC irradiation. (B) The kinetics of UVC—induced NER—repaired adducts using alkaline comet assay and (C) total amounts of DNA damage expressed as AUC for DNA damage during the whole experiment (0–6 h). (D) Redox status and (E) AP-sites at different time points after UVC irradiation. (F) Total amounts of AP-sites expressed as AUC. Error bars represent SD; * $p < 0.05$, ** $p < 0.01$, and *** $p < 0.001$. The experiments shown were based on a minimum of three independent repeats.

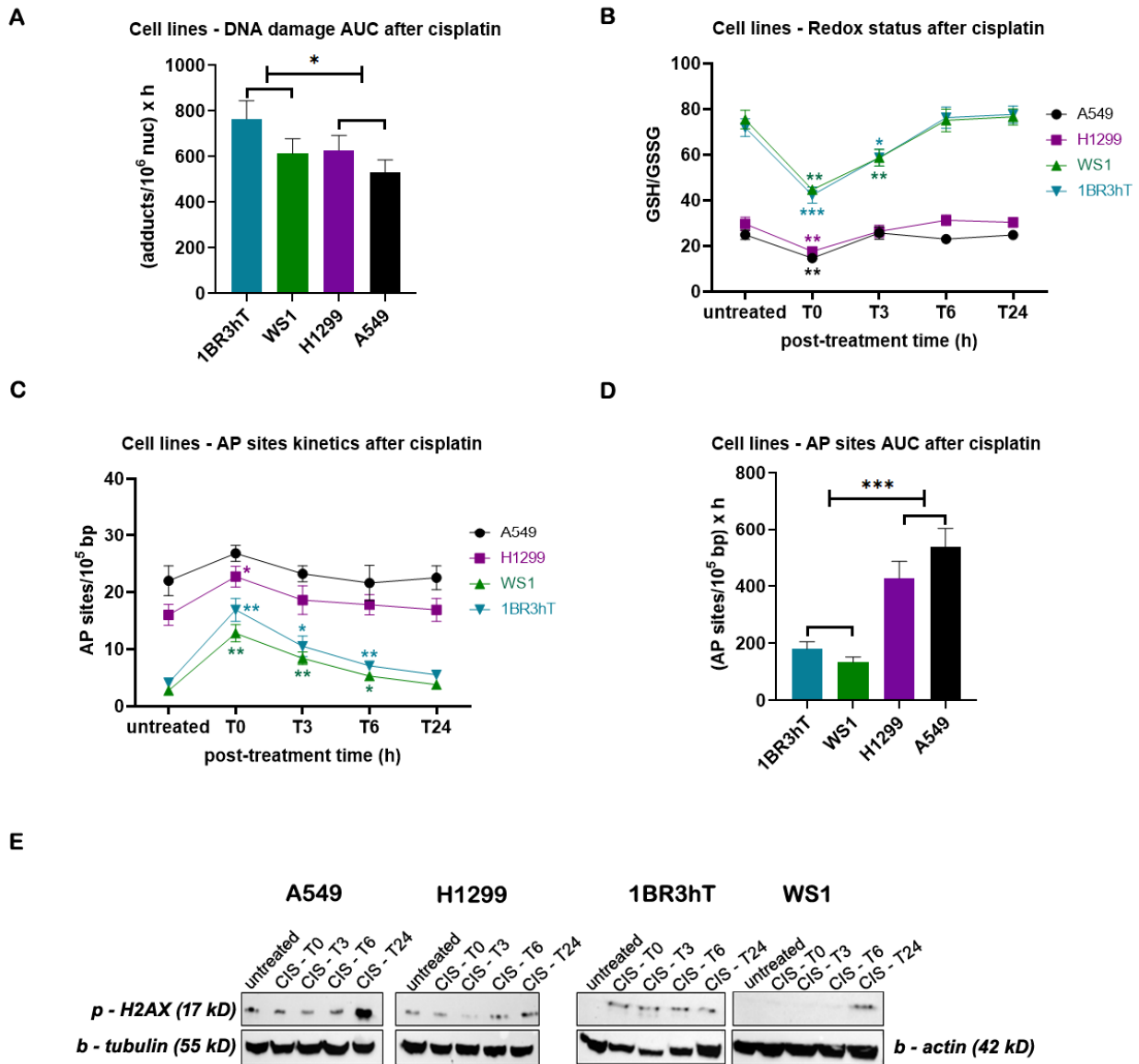


Figure 3. DDR-associated parameters in cell lines following cisplatin treatment. (A) The total amounts of cisplatin-induced ICLs expressed as AUC for DNA damage. (B) Redox status and (C) AP-sites at different time points after cisplatin treatment. (D) Total amounts of AP-sites expressed as AUC. (E) Western blots showing the amounts of γ H2AX at different time point after cisplatin treatment. β -tubulin and β -actin were used as loading controls. Error bars represent SD; * $p < 0.05$, ** $p < 0.01$, and *** $p < 0.001$. The experiments shown were based on a minimum of three independent repeats.

3.2. DDR Signals in PBMCs from Patients with Lung Cancer

To test the hypothesis that DDR-associated signals and redox status are implicated in the response to platinum-based chemotherapy, changes in the DDR parameters and the GSH/GSSG ratios were evaluated in PBMCs from 20 healthy controls and 32 patients with lung cancer at baseline (17 responders and 15 non-responders to subsequent platinum-based chemotherapy).

Firstly, factors implicated in the formation of DNA damage were evaluated. In line with our previous data [43] and the cell lines' results, compared with PBMCs from healthy individuals, patients' cells exhibited significantly lower GSH/GSSG ratios (Figure 4A) and higher burdens of AP-sites (Figure 4B) at baseline (all $p < 0.001$). Interestingly, responders to subsequent chemotherapy were characterized by a significantly lower baseline GSH/GSSG ratio and higher baseline levels of AP-sites compared to non-responders (all $p < 0.001$;

Figure 4A,B). In addition, the lowest doses of cisplatin required for the induction of apoptosis at 24 h were significantly higher in PBMCs from patients at baseline compared with healthy controls (all $p < 0.001$), indicating that patients' PBMCs exhibited significantly decreased apoptosis rates (Figure 4C). In particular, non-responders at baseline exhibited significantly lower apoptotic rates than responders, as their samples required the highest cisplatin dose for apoptosis induction (all $p < 0.001$; Figure 4C).

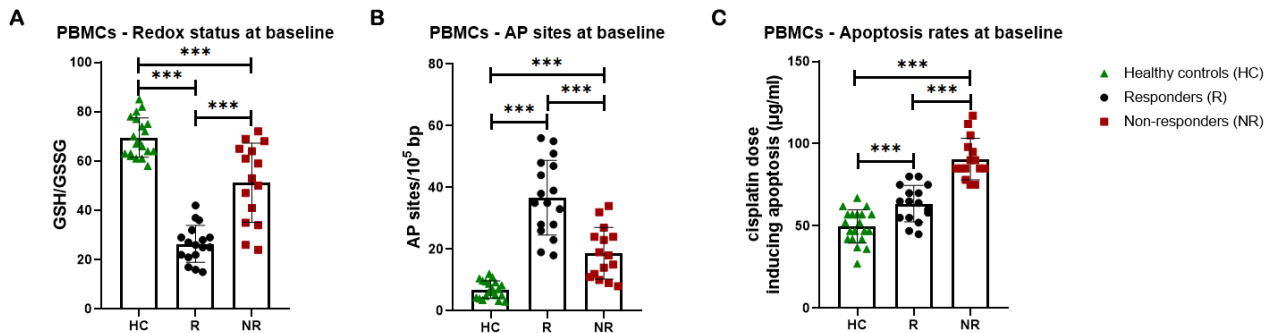


Figure 4. DDR-associated parameters in PBMCs at baseline (A) Bar charts showing the endogenous/baseline redox status expressed by the GSH/GSSG ratio at PBMCs from healthy controls (HCs) and patients, responders (Rs), and non-responders (NRs) to subsequent chemotherapy-based treatment. (B) Baseline AP-sites levels for PBMCs. (C) Apoptosis rates at baseline for PBMCs. Error bars represent SD; *** $p < 0.001$. The experiments shown were based on a minimum of three independent repeats.

Subsequently, NER efficiency was analyzed in PBMCs following irradiation with 5 J/m² UVC. In line with our previous data [43] and the cell lines' results, significantly lower NER capacity was observed in patients with lung cancer compared with healthy controls, resulting in higher accumulation of NER-repaired lesions in patients' PBMCs ($p < 0.01$). Intriguingly, patients who responded to subsequent platinum chemotherapy showed significantly lower rates of NER compared with both non-responders and healthy controls, resulting in a significantly higher DNA damage burden in responders' cells (all $p < 0.001$; Figure 5A,B). Non-responders exhibit similar DNA damage levels to healthy controls, suggesting that impaired NER efficiency might be crucial to chemotherapy response.

In addition, we found that, in a 6 h time frame after UVC irradiation, patients' samples were characterized by a lower GSH/GSSG ratio and higher UVC-induced AP-sites than healthy controls, with responders showing the lowest GSH/GSSG ratio and the highest levels of AP-sites (all $p < 0.01$; Figure 5C–E).

Next, to investigate the ICL repair efficiency, PBMCs were treated ex vivo with 5 µg/mL cisplatin for 3 h, and the ICL levels were analyzed up to 24 h after treatment. We found that patients with lung cancer showed significantly lower ICL repair capacity than healthy controls, as depicted by higher DNA damage burden after cisplatin treatment ($p < 0.001$). In line with the NER capacity, responders' cells showed much lower ICL repair capacity than non-responders, resulting in significantly higher accumulation of ICLs in responders' PBMCs ($p < 0.001$, Figure 6A,B). Once again, non-responders show DNA damage levels equivalent to the ones of healthy controls. In accordance with previous data showing that there is a correlation between the cytotoxicity of bifunctional drugs and the ICL burden (expressed as AUC) [44], we found that the individual levels of cisplatin-induced ICLs (expressed as AUC) correlate with the corresponding apoptosis rates (Figure S1). The GSH/GSSG ratio and AP-sites within 24 h after cisplatin treatment were also evaluated. Significantly lower GSH/GSSG ratio and higher levels of AP-sites were obtained in patients' samples compared with healthy controls, with responders presenting significantly diminished the GSH/GSSG ratio and augmented levels of AP-sites compared to non-responders (all $p < 0.001$; Figure 6C–E).

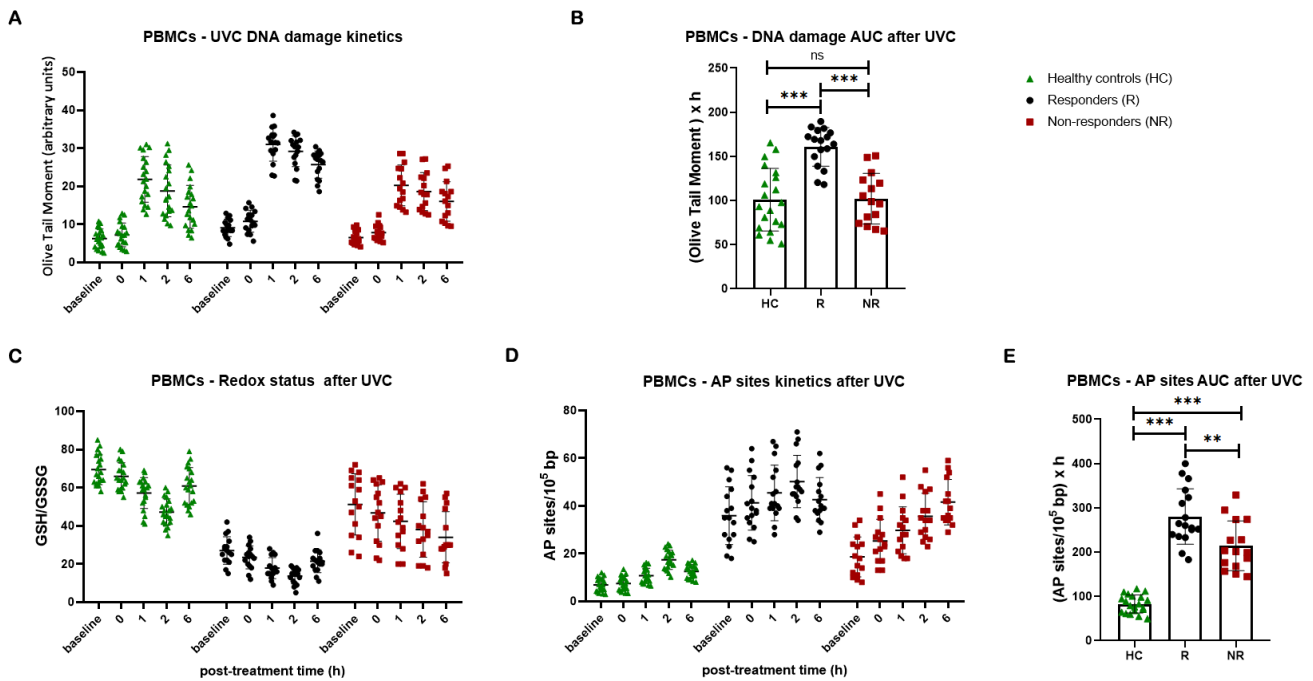


Figure 5. DDR signals in PBMCs after UVC irradiation. (A) The kinetics of UVC-induced DNA lesions using alkaline comet assay and (B) total amounts of DNA lesions expressed as AUC in PBMCs from healthy controls and patients with lung cancer. (C) Redox status and (D) AP-sites at different time points after UVC irradiation of PBMCs. (E) Total amounts of AP-sites expressed as AUC. Error bars represent SD; ** $p < 0.01$, and *** $p < 0.001$. The experiments shown were based on a minimum of three independent repeats.

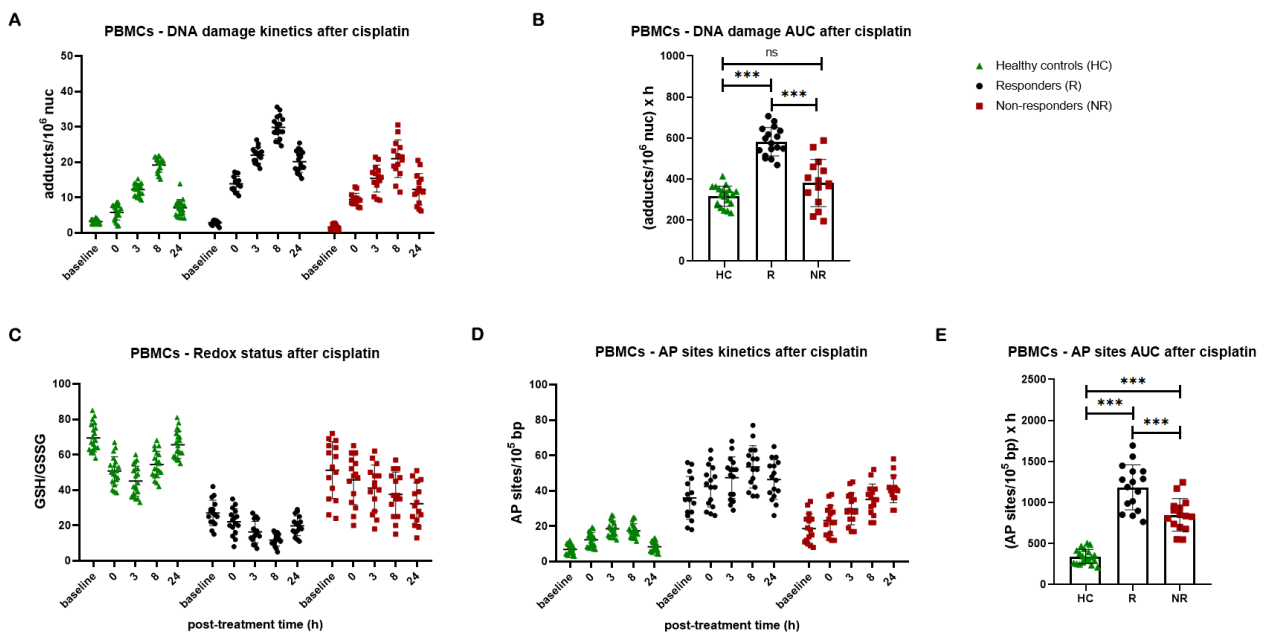


Figure 6. DNA damage response parameters in PBMCs after the ex vivo cisplatin treatment. (A) The kinetics of cisplatin-induced ICLs and (B) total amounts of ICLs expressed as AUC for DNA damage in PBMCs from healthy controls and patients with lung cancer. (C) Redox status and (D) AP-sites at baseline and after cisplatin treatment. (E) Total amounts of AP-sites expressed as AUC in PBMCs. Error bars represent SD; *** $p < 0.001$. The experiments shown were based on a minimum of three independent repeats.

4. Discussion

The development of drug resistance poses a significant challenge to platinum-based chemotherapy, a crucial treatment regimen employed in the therapeutic management of several malignancies, including lung cancer [45]. Cisplatin's mechanism of action involves its binding to DNA and the creation of monoadducts, mostly through covalent interactions with guanine's N7 position. Through a second covalent binding, this monoadduct transforms into a DNA cross-link, which can occur either on the opposite strand (ICL; inter-strand; the most cytotoxic) or on the same DNA strand (intra-strand). Notably, cisplatin does not directly produce double-strand breaks [46]. However, it may still induce double-strand damage when replication forks encounter obstacles to their progression. Indeed, in dividing cells, during the ICL repair, ERCC1-XPF endonuclease makes two incisions on either side of the crosslink in order to release the covalent bond between the two DNA strands. This unhooking event then creates a resection gap, which serves as an appropriate substrate for homologous recombination [47–49]. Interestingly, ICL can block the progression of the DNA replication fork, which may lead to the creation of a DNA DSB. In contrast to the direct DSBs that are caused by ionizing radiation, which are typically repaired by non-homologous end joining, these ICL-induced DSBs are repaired by homologous recombination repair [48,49].

Phosphorylation of histone H2AX at position Ser139 (γ H2AX) has become a tool to monitor double-strand breaks [50]. Phosphorylation usually happens immediately after the formation of DSBs. However, Olive et al. [51] reported that after exposure to cisplatin, phosphorylation was delayed, reaching maximal levels 6–18 h after drug treatment. They also observed that the time of peak γ H2AX levels was cisplatin-dose dependent. This situation was further complicated by the necessity for drug-damaged cells to progress into the S phase. Notably, they found that measurement of γ H2AX foci at 24 h post-treatment could serve as a valuable marker of cellular response to cisplatin-induced death. In line with these data, herein, we found that γ H2AX protein levels appear shortly after treatment and increase over time, reaching maximal levels within 24 h. Oxidative stress and ROS generation are also linked to cisplatin's cytotoxic effects [21,24–27]. Therefore, in this study we tested the hypothesis that redox status and DDR-related signals measured in PBMCs from patients with lung cancer might correlate with therapeutic response to platinum-based therapy.

Firstly, the redox status, expressed as the GSH/GSSG ratio, was assessed. In line with previous studies showing that in cancer cells a number of variables, such as hypoxia, aerobic glycolysis, and oncogene activation, disrupt the redox balance and lead to ROS accumulation, we found that PBMCs from patients with lung cancer showed lower a GSH/GSSG ratio than healthy controls. Prior research has demonstrated a robust association between lung cancer and redox imbalance [52]. In fact, patients with lung cancer had higher levels of oxidative stress biomarkers, including 8-oxodG and malondialdehyde, as well as reduced levels of antioxidative biomarkers, such as red cell superoxide dismutase and glutathione peroxidase activities [53]. Of note, chronic inflammation of the lung tissue is known to be associated with lung cancer [54]. Interestingly, cigarette smoke is known to increase inflammation by raising the number of inflammatory immune cells in the airways and causing the release of proinflammatory cytokines including GM-CSF, TNF- α , IL-1, IL-6, and IL-8 [55]. Furthermore, DNA damage can also result in elevated ROS, which can further exacerbate oxidative damage, creating a vicious cycle and raising the burden of DNA damage. Given that the oxidative damage caused by ROS within cells leads to modifications of DNA bases, the greater numbers of AP-sites observed in the patients with lung cancer examined herein may be explained by increased oxidative stress.

Importantly, significant differences in the redox status were found between patients sensitive or resistant to subsequent platinum-based therapy. Indeed, we found that PBMCs from responders are characterized by lower baseline and cisplatin-induced GSH/GSSG ratios compared with patients who are non-responders. Previous studies have shown that the increase in cellular GSH plays a crucial role in cisplatin resistance because of its

detoxification effect [56]. That is, before attaching to DNA, many platinum molecules form a Pt(GS)₂ conjugate with GSH, which is subsequently removed from the cell. Even though this conjugation may deplete the antioxidant reservoir of the cells and result in oxidative stress, high levels of GSH lower the quantity of reactive cisplatin, thus limiting its anticancer effectiveness [57]. Therefore, it would be expected that an increase in GSH synthesis in cancer cells will cause resistance to platinum-based regimens.

Since the generation of ROS following treatment with many anticancer drugs may augment the treatment efficacy, there is growing interest in combining ROS-inducing agents with chemotherapy [58–60]. Indeed, pro-oxidative anticancer drugs, including curcumin and its derivatives, Choline Tetrathiomolybdate (ATN-224), 15-Deoxy-Delta-12,14-prostaglandin J₂ (15d-PGJ₂), 2-Methoxyoestradiol, and carnosol, are in various stages of research and development [61]. On the other hand, oxidative stress disrupts cellular processes, including the regulation of the cell cycle, apoptosis, and DNA repair mechanisms that are essential for antineoplastic agents to exert their maximum cytotoxicity on cancer cells [62]. This results in the increased lipid peroxidation products, the decrease in blood plasma's capacity to trap radicals, the reduction of the plasma levels of beta-carotene, vitamin C, and vitamin E, the induction of oxidative DNA damage, as well as the decrease in tissue glutathione levels after chemotherapy [63]. Thus, oxidative stress can also adversely affect normal tissues that undergo rapid proliferation, such as the heart, liver, lungs, kidneys, and gastrointestinal system [64]. Moreover, other adverse events, such as tumor cell adaptation to oxidative stress and cell cycle changes by oxidative stress, decrease the effectiveness of chemotherapy and induce cancer metastasis and recurrence [65]. Interestingly, combination treatment including antioxidants to reduce the side effects of chemotherapy might potentially decrease the efficacy of anticancer agents [66].

Since cisplatin cytotoxicity is mainly due to its ability to cause DNA damage, DNA repair capacity is expected to be one of the most important cisplatin-resistance mechanisms. In this study, we found that patients with lung cancer exhibited decreased NER and ICL repair capacities compared with healthy controls. NER pathway is an important repair mechanism, as it is responsible for the repair of a variety of DNA lesions caused by multiple factors such as UV light, ionizing irradiation, ROS, and chemotherapeutic drugs, including cisplatin [67]. Evidence has suggested that this pathway may be inhibited in lung cells exposed to tobacco smoke [68], with a recent study showing correlations between NER mutations and smoking status in patients with NSCLC [69]. Specifically, an ERCC1 genetic polymorphism was found to be increased in patients who are heavy smokers with NSCLC [69]. ERCC1 is known to be indispensable for the NER pathway, and it has been previously implicated with chemoresistance in lung adenocarcinoma [70]. Moreover, our previous study has shown deregulation of the genes encoding the NER-related molecular components of the heterodimer DDB complex (DDB1 and DDB2) in patients with lung cancer [52]. In line with the NER results, herein we found that PBMCs derived from patients with lung cancer are characterized by decreased ICL repair capacities. In addition, we found reduced apoptosis rates in patients with lung cancer. These results are in accordance with previous data showing that the absence of apoptotic regulation prolongs the life of cancer cells and provides more time for mutations to accumulate, which might enhance invasiveness as the tumor grows, deregulate differentiation pathways, and promote angiogenesis [43]. Corresponding results on most DDR-related parameters were also obtained in cell line experiments, thus further validating the broad applicability of our results. Interestingly, lung cancer cell lines additionally showed higher endogenous/baseline DNA damage (both single- and double-strand breaks) compared to normal fibroblasts, partly due to the elevated levels of oxidative stress that were found in malignant cell lines.

Importantly, significant differences in the NER and ICL repair capacities were observed between lung patients sensitive or resistant to subsequent platinum-based therapy. Indeed, following treatment with UVC or cisplatin, limited lesion accumulation in non-responders' PBMCs was found, probably emerging from excessive DNA repair activity of both NER and ICL repair mechanisms, resulting in strong resistance to apoptosis in non-responder

samples. These results are in line with previous studies in solid tumors, including lung cancer [71–74], head and neck cancer [75–78], ovarian cancer [52,79,80], testicular cancer [79], and colorectal cancer [22], as well as in hematologic malignancies [44,81–84]. These results suggest that it might be possible to predict chemotherapy outcomes by measuring DDR signals in PBMCs derived from patients with cancer.

A limitation of the present study is that we measured DDR-related parameters in the whole PBMC fraction derived from patients with lung cancer. Since PBMCs are not a homogeneous cell population but are composed of various cell types, such as T cells (45–70%), B cells (5–10%), monocytes (10–30%), natural killer cells (NKs; 5–20%), and dendritic cells (0.5–2%) [85], it is important to determine if subpopulations of PBMCs might vary in their response to DNA damage. Therefore, analyzing DDR-associated parameters in the subpopulations of PBMCs from patients with lung cancer with different response rates is an important direction for our future research.

5. Conclusions

In order to protect against genotoxic effects, cells have developed a number of genome-protection mechanisms, which are collectively referred to as the DNA damage response network. Interestingly, dysregulation of this system has been linked to the onset and progression of multiple diseases, such as cancer, as well as the response to therapies that cause damage to DNA. In addition, multiple diseases, such as cancer, are caused by disruption of redox homeostasis, which is necessary for human health, with oxidative stress also playing a crucial role in the cytotoxicity of platinum drugs. Therefore, herein we investigated the relationship between the therapeutic benefit of platinum-based regimens, the redox status, and the DDR-related signals of PBMCs derived from patients with lung cancer at baseline. We found that redox status expressed as the GSH/GSSG ratio, the apurinic/aprimidinic sites, the DNA repair capacity of critical DNA repair mechanisms, namely NER and ICL repair, and the apoptosis rates display significant differences among patients and correlate with the clinical responses to platinum-based therapy. These findings might be exploited as tools to design novel non-invasive predictive biomarkers and might contribute to the identification of patients with lung cancer who are more likely to benefit from this type of therapy.

Supplementary Materials: The following supporting information can be downloaded at <https://www.mdpi.com/article/10.3390/cancers16244218/s1>: Figure S1: Correlation between the cisplatin-induced ICL burden and the apoptosis rates.

Author Contributions: Conceptualization, D.M., D.T.S., K.N.S. and V.L.S.; data curation, D.M. and V.L.S.; formal analysis, D.M. and V.L.S.; funding acquisition, D.M., D.T.S. and K.N.S.; investigation, D.M., A.G., D.T.S. and V.L.S.; project administration, V.L.S.; resources, V.L.S.; supervision, K.N.S. and V.L.S.; validation, D.M., D.T.S., C.P., K.N.S. and V.L.S.; visualization, D.M. and V.L.S.; writing—original draft, D.M. and V.L.S.; writing—review and editing, D.M., A.G., D.T.S., C.P., K.N.S. and V.L.S. All authors will be updated at each stage of manuscript processing, including submission, revision, and revision reminder, via emails from our system or the assigned Assistant Editor. All authors have read and agreed to the published version of the manuscript.

Funding: This work was supported by the Hellenic Society of Medical Oncology (HeSMO) (8177/10-02-2021 and 9597/19-6-2024 research grants).

Institutional Review Board Statement: The study was conducted in accordance with the Declaration of Helsinki, and approved by the Institutional Review Board of Sotiria Hospital (protocol Nos. 15627/11-6-2020 and 25950/10-10-2022).

Informed Consent Statement: Informed consent was obtained from all subjects involved in the study.

Data Availability Statement: The data presented in this study are available by specific request to the corresponding author.

Acknowledgments: We thank Athanassios Kotsinas, Maria Fousteri, and Panagiotis Georgiadis for providing cell lines.

Conflicts of Interest: The authors declare no conflicts of interest.

References

1. Thai, A.A.; Solomon, B.J.; Sequist, L.V.; Gainor, J.F.; Heist, R.S. Lung Cancer. *Lancet* **2021**, *398*, 535–554. [[CrossRef](#)] [[PubMed](#)]
2. Li, Y.; Yan, B.; He, S. Advances and Challenges in the Treatment of Lung Cancer. *Biomed. Pharmacother.* **2023**, *169*, 115891. [[CrossRef](#)]
3. Sears, C.R.; Mazzone, P.J. Biomarkers in Lung Cancer. *Clin. Chest Med.* **2020**, *41*, 115–127. [[CrossRef](#)] [[PubMed](#)]
4. Li, Y.; Hecht, S.S. Carcinogenic Components of Tobacco and Tobacco Smoke: A 2022 Update. *Food Chem. Toxicol.* **2022**, *165*, 113179. [[CrossRef](#)]
5. Corrales, L.; Rosell, R.; Cardona, A.F.; Martín, C.; Zatarain-Barrón, Z.L.; Arrieta, O. Lung Cancer in Never Smokers: The Role of Different Risk Factors Other than Tobacco Smoking. *Crit. Rev. Oncol./Hematol.* **2020**, *148*, 102895. [[CrossRef](#)]
6. Laguna, J.C.; García-Pardo, M.; Alessi, J.; Barrios, C.; Singh, N.; Al-Shamsi, H.O.; Loong, H.; Ferriol, M.; Recondo, G.; Mezquita, L. Geographic Differences in Lung Cancer: Focus on Carcinogens, Genetic Predisposition, and Molecular Epidemiology. *Ther. Adv. Med. Oncol.* **2024**, *16*, 17588359241231260. [[CrossRef](#)]
7. Cadet, J.; Wagner, J.R. DNA Base Damage by Reactive Oxygen Species, Oxidizing Agents, and UV Radiation. *Cold Spring Harb. Perspect. Biol.* **2013**, *5*, a012559. [[CrossRef](#)]
8. Chatterjee, N.; Walker, G.C. Mechanisms of DNA Damage, Repair, and Mutagenesis. *Environ. Mol. Mutagen.* **2017**, *58*, 235–263. [[CrossRef](#)]
9. Van Houten, B.; Santa-Gonzalez, G.A.; Camargo, M. DNA Repair after Oxidative Stress: Current Challenges. *Curr. Opin. Toxicol.* **2018**, *7*, 9–16. [[CrossRef](#)]
10. Ganai, R.A.; Johansson, E. DNA Replication—A Matter of Fidelity. *Mol. Cell* **2016**, *62*, 745–755. [[CrossRef](#)]
11. Tubbs, A.; Nussenzweig, A. Endogenous DNA Damage as a Source of Genomic Instability in Cancer. *Cell* **2017**, *168*, 644–656. [[CrossRef](#)] [[PubMed](#)]
12. Cheung, E.C.; Vousden, K.H. The Role of ROS in Tumour Development and Progression. *Nat. Rev. Cancer* **2022**, *22*, 280–297. [[CrossRef](#)] [[PubMed](#)]
13. Yang, S.; Lian, G. ROS and Diseases: Role in Metabolism and Energy Supply. *Mol. Cell. Biochem* **2020**, *467*, 1–12. [[CrossRef](#)]
14. Bansal, A.; Simon, M.C. Glutathione Metabolism in Cancer Progression and Treatment Resistance. *J. Cell Biol.* **2018**, *217*, 2291–2298. [[CrossRef](#)]
15. Park, H.S.; Kim, S.R.; Lee, Y.C. Impact of Oxidative Stress on Lung Diseases. *Respirology* **2009**, *14*, 27–38. [[CrossRef](#)]
16. Dizdaroglu, M. Oxidatively Induced DNA Damage: Mechanisms, Repair and Disease. *Cancer Lett.* **2012**, *327*, 26–47. [[CrossRef](#)]
17. Renaudin, X. Reactive Oxygen Species and DNA Damage Response in Cancer. In *International Review of Cell and Molecular Biology*; Elsevier: Amsterdam, The Netherlands, 2021; Volume 364, pp. 139–161. ISBN 978-0-323-85561-7.
18. Souliotis, V.L.; Vlachogiannis, N.I.; Pappa, M.; Argyriou, A.; Ntouros, P.A.; Sfikakis, P.P. DNA Damage Response and Oxidative Stress in Systemic Autoimmunity. *Int. J. Mol. Sci.* **2019**, *21*, 55. [[CrossRef](#)]
19. Zhao, H.; Shen, J.; Deininger, P.; Hunt, J.D. Abasic Sites and Survival in Resected Patients with Non-Small Cell Lung Cancer. *Cancer Lett.* **2007**, *246*, 47–53. [[CrossRef](#)]
20. Long, K.; Gu, L.; Li, L.; Zhang, Z.; Li, E.; Zhang, Y.; He, L.; Pan, F.; Guo, Z.; Hu, Z. Small-Molecule Inhibition of APE1 Induces Apoptosis, Pyroptosis, and Necroptosis in Non-Small Cell Lung Cancer. *Cell Death Dis.* **2021**, *12*, 503. [[CrossRef](#)]
21. Berndtsson, M.; Hägg, M.; Panaretakis, T.; Havelka, A.M.; Shoshan, M.C.; Linder, S. Acute Apoptosis by Cisplatin Requires Induction of Reactive Oxygen Species but Is Not Associated with Damage to Nuclear DNA. *Int. J. Cancer* **2007**, *120*, 175–180. [[CrossRef](#)]
22. Chen, W.; Lian, W.; Yuan, Y.; Li, M. The Synergistic Effects of Oxaliplatin and Piperlongumine on Colorectal Cancer Are Mediated by Oxidative Stress. *Cell Death Dis.* **2019**, *10*, 600. [[CrossRef](#)] [[PubMed](#)]
23. Van Loenhout, J.; Peeters, M.; Bogaerts, A.; Smits, E.; Deben, C. Oxidative Stress-Inducing Anticancer Therapies: Taking a Closer Look at Their Immunomodulating Effects. *Antioxidants* **2020**, *9*, 1188. [[CrossRef](#)] [[PubMed](#)]
24. Cadoni, E.; Valletta, E.; Caddeo, G.; Isaia, F.; Cabiddu, M.G.; Vascellari, S.; Pivetta, T. Competitive Reactions among Glutathione, Cisplatin and Copper-Phenanthroline Complexes. *J. Inorg. Biochem.* **2017**, *173*, 126–133. [[CrossRef](#)] [[PubMed](#)]
25. Jamali, B.; Nakhjavani, M.; Hosseinzadeh, L.; Amidi, S.; Nikounezhad, N.; Shirazi, F.H. Intracellular GSH Alterations and Its Relationship to Level of Resistance Following Exposure to Cisplatin in Cancer Cells. *Iran. J. Pharm. Sci.* **2015**, *14*, 513–519.
26. Li, S.; Li, C.; Jin, S.; Liu, J.; Xue, X.; Eltahan, A.S.; Sun, J.; Tan, J.; Dong, J.; Liang, X.-J. Overcoming Resistance to Cisplatin by Inhibition of Glutathione S-Transferases (GSTs) with Ethacraplatin Micelles in Vitro and in Vivo. *Biomaterials* **2017**, *144*, 119–129. [[CrossRef](#)]
27. Chen, H.H.W.; Kuo, M.T. Role of Glutathione in the Regulation of Cisplatin Resistance in Cancer Chemotherapy. *Metal-Based Drugs* **2010**, *2010*, 430939. [[CrossRef](#)]
28. Kasherman, Y.; Sturup, S.; Gibson, D. Is Glutathione the Major Cellular Target of Cisplatin? A Study of the Interactions of Cisplatin with Cancer Cell Extracts. *J. Med. Chem.* **2009**, *52*, 4319–4328. [[CrossRef](#)]
29. Silva, M.M.; Rocha, C.R.R.; Kinker, G.S.; Pelegrini, A.L.; Menck, C.F.M. The Balance between NRF2/GSH Antioxidant Mediated Pathway and DNA Repair Modulates Cisplatin Resistance in Lung Cancer Cells. *Sci. Rep.* **2019**, *9*, 17639. [[CrossRef](#)]

30. Vascellari, S.; Valletta, E.; Perra, D.; Pinna, E.; Serra, A.; Isaia, F.; Pani, A.; Pivetta, T. Cisplatin, Glutathione and the Third Wheel: A Copper-(1,10-Phenanthroline) Complex Modulates Cisplatin–GSH Interactions from Antagonism to Synergism in Cancer Cells Resistant to Cisplatin. *RSC Adv.* **2019**, *9*, 5362–5376. [[CrossRef](#)]
31. Hannon Barroeta, P.; O’Sullivan, M.J.; Zisterer, D.M. The Role of the Nrf2/GSH Antioxidant System in Cisplatin Resistance in Malignant Rhabdoid Tumours. *J. Cancer Res. Clin. Oncol.* **2023**, *149*, 8379–8391. [[CrossRef](#)]
32. Black, H.; Mills, K. The DNA Damage Repair Response. *Clin. Oncol.* **2020**, *3*, 1–14. [[CrossRef](#)]
33. Jackson, S.P.; Bartek, J. The DNA-Damage Response in Human Biology and Disease. *Nature* **2009**, *461*, 1071–1078. [[CrossRef](#)] [[PubMed](#)]
34. Hsiehchen, D.; Hsieh, A.; Samstein, R.M.; Lu, T.; Beg, M.S.; Gerber, D.E.; Wang, T.; Morris, L.G.T.; Zhu, H. DNA Repair Gene Mutations as Predictors of Immune Checkpoint Inhibitor Response beyond Tumor Mutation Burden. *Cell Rep. Med.* **2020**, *1*, 100034. [[CrossRef](#)] [[PubMed](#)]
35. Xu, Y.; Nowsheen, S.; Deng, M. DNA Repair Deficiency Regulates Immunity Response in Cancers: Molecular Mechanism and Approaches for Combining Immunotherapy. *Cancers* **2023**, *15*, 1619. [[CrossRef](#)] [[PubMed](#)]
36. Härtlova, A.; Erttmann, S.F.; Raffi, F.A.; Schmalz, A.M.; Resch, U.; Anugula, S.; Lienenklaus, S.; Nilsson, L.M.; Kröger, A.; Nilsson, J.A.; et al. DNA Damage Primes the Type I Interferon System via the Cytosolic DNA Sensor STING to Promote Anti-Microbial Innate Immunity. *Immunity* **2015**, *42*, 332–343. [[CrossRef](#)]
37. Kwon, J.; Bakhoun, S.F. The Cytosolic DNA-Sensing cGAS–STING Pathway in Cancer. *Cancer Discov.* **2020**, *10*, 26–39. [[CrossRef](#)]
38. Pilger, D.; Seymour, L.W.; Jackson, S.P. Interfaces between Cellular Responses to DNA Damage and Cancer Immunotherapy. *Genes Dev.* **2021**, *35*, 602–618. [[CrossRef](#)]
39. Rossi, A.; Di Maio, M. Platinum-Based Chemotherapy in Advanced Non-Small-Cell Lung Cancer: Optimal Number of Treatment Cycles. *Expert Rev. Anticancer Ther.* **2016**, *16*, 653–660. [[CrossRef](#)]
40. Larminat, F.; Zhen, W.; Bohr, V.A. Gene-Specific DNA Repair of Interstrand Cross-Links Induced by Chemotherapeutic Agents Can Be Preferential. *J. Biol. Chem.* **1993**, *268*, 2649–2654. [[CrossRef](#)]
41. Souliotis, V.L.; Dimopoulos, M.A.; Sfrikakis, P.P. Gene-Specific Formation and Repair of DNA Monoadducts and Interstrand Cross-Links after Therapeutic Exposure to Nitrogen Mustards. *Clin. Cancer Res.* **2003**, *9*, 4465–4474.
42. Scharer, O.D. Nucleotide Excision Repair in Eukaryotes. *Cold Spring Harb. Perspect. Biol.* **2013**, *5*, a012609. [[CrossRef](#)] [[PubMed](#)]
43. Stefanou, D.T.; Kouvela, M.; Stellas, D.; Voutetakis, K.; Papadodima, O.; Syrigos, K.; Souliotis, V.L. Oxidative Stress and Deregulated DNA Damage Response Network in Lung Cancer Patients. *Biomedicines* **2022**, *10*, 1248. [[CrossRef](#)] [[PubMed](#)]
44. Gkotszamanidou, M.; Terpos, E.; Bamia, C.; Munshi, N.C.; Dimopoulos, M.A.; Souliotis, V.L. DNA Repair of Myeloma Plasma Cells Correlates with Clinical Outcome: The Effect of the Nonhomologous End-Joining Inhibitor SCR7. *Blood* **2016**, *128*, 1214–1225. [[CrossRef](#)] [[PubMed](#)]
45. Shahlaei, M. Platinum-Based Drugs in Cancer Treatment: Expanding Horizons and Overcoming Resistance. *J. Mol. Struct.* **2024**, *1301*, 137366. [[CrossRef](#)]
46. De Silva, I.U. Defects in Interstrand Cross-Link Uncoupling Do Not Account for the Extreme Sensitivity of ERCC1 and XPF Cells to Cisplatin. *Nucleic Acids Res.* **2002**, *30*, 3848–3856. [[CrossRef](#)]
47. Rothfuss, A.; Grompe, M. Repair Kinetics of Genomic Interstrand DNA Cross-Links: Evidence for DNA Double-Strand Break-Dependent Activation of the Fanconi Anemia/BRCA Pathway. *Mol. Cell. Biol.* **2004**, *24*, 123–134. [[CrossRef](#)]
48. Dronkert, M.L.G.; Kanaar, R. Repair of DNA Interstrand Cross-Links. *Mutat. Res./DNA Repair* **2001**, *486*, 217–247. [[CrossRef](#)]
49. Silva, I.U.D.; Mchugh, P.J.; Clingen, P.H.; Hartley, J.A. Defining the Roles of Nucleotide Excision Repair and Recombination in the Repair of DNA Interstrand Cross-Links in Mammalian Cells. *Mol. Cell. Biol.* **2000**, *20*, 7980–7990. [[CrossRef](#)]
50. Ivashkevich, A.; Redon, C.E.; Nakamura, A.J.; Martin, R.F.; Martin, O.A. Use of the γ -H2AX Assay to Monitor DNA Damage and Repair in Translational Cancer Research. *Cancer Lett.* **2012**, *327*, 123–133. [[CrossRef](#)]
51. Olive, P.L.; Banáth, J.P. Kinetics of H2AX Phosphorylation after Exposure to Cisplatin. *Cytom. Part B Clin.* **2009**, *76B*, 79–90. [[CrossRef](#)]
52. Stefanou, D.T.; Souliotis, V.L.; Zakopoulou, R.; Liontos, M.; Bamias, A. DNA Damage Repair: Predictor of Platinum Efficacy in Ovarian Cancer? *Biomedicines* **2021**, *10*, 82. [[CrossRef](#)] [[PubMed](#)]
53. Peddireddy, V.; Siva Prasad, B.; Gundimeda, S.D.; Penagaluru, P.R.; Mundluru, H.P. Assessment of 8-Oxo-7, 8-Dihydro-2’-Deoxyguanosine and Malondialdehyde Levels as Oxidative Stress Markers and Antioxidant Status in Non-Small Cell Lung Cancer. *Biomarkers* **2012**, *17*, 261–268. [[CrossRef](#)] [[PubMed](#)]
54. Qian, S.; Golubnitschaja, O.; Zhan, X. Chronic Inflammation: Key Player and Biomarker-Set to Predict and Prevent Cancer Development and Progression Based on Individualized Patient Profiles. *EPMA J.* **2019**, *10*, 365–381. [[CrossRef](#)]
55. Lu, L.-M.; Zavitz, C.C.J.; Chen, B.; Kianpour, S.; Wan, Y.; Stämpfli, M.R. Cigarette Smoke Impairs NK Cell-Dependent Tumor Immune Surveillance. *J. Immunol.* **2007**, *178*, 936–943. [[CrossRef](#)]
56. Han, Y.; Yin, W.; Li, J.; Zhao, H.; Zha, Z.; Ke, W.; Wang, Y.; He, C.; Ge, Z. Intracellular Glutathione-Depleting Polymeric Micelles for Cisplatin Prodrug Delivery to Overcome Cisplatin Resistance of Cancers. *J. Control. Release* **2018**, *273*, 30–39. [[CrossRef](#)]
57. Galluzzi, L.; Senovilla, L.; Vitale, I.; Michels, J.; Martins, I.; Kepp, O.; Castedo, M.; Kroemer, G. Molecular Mechanisms of Cisplatin Resistance. *Oncogene* **2012**, *31*, 1869–1883. [[CrossRef](#)]
58. Li, X.; Hou, Y.; Zhao, J.; Li, J.; Wang, S.; Fang, J. Combination of Chemotherapy and Oxidative Stress to Enhance Cancer Cell Apoptosis. *Chem. Sci.* **2020**, *11*, 3215–3222. [[CrossRef](#)]

59. Kim, S.J.; Kim, H.S.; Seo, Y.R. Understanding of ROS-Inducing Strategy in Anticancer Therapy. *Oxid. Med. Cell. Longev.* **2019**, *2019*, 1–12. [[CrossRef](#)]
60. Liu, T.-I.; Lu, T.-Y.; Yang, Y.-C.; Chang, S.-H.; Chen, H.-H.; Lu, I.-L.; Sabu, A.; Chiu, H.-C. New Combination Treatment from ROS-Induced Sensitized Radiotherapy with Nanophototherapeutics to Fully Eradicate Orthotopic Breast Cancer and Inhibit Metastasis. *Biomaterials* **2020**, *257*, 120229. [[CrossRef](#)]
61. Nizami, Z.N.; Aburawi, H.E.; Semlali, A.; Muhammad, K.; Iratni, R. Oxidative Stress Inducers in Cancer Therapy: Preclinical and Clinical Evidence. *Antioxidants* **2023**, *12*, 1159. [[CrossRef](#)]
62. Iqbal, M.J.; Kabeer, A.; Abbas, Z.; Siddiqui, H.A.; Calina, D.; Sharifi-Rad, J.; Cho, W.C. Interplay of Oxidative Stress, Cellular Communication and Signaling Pathways in Cancer. *Cell Commun. Signal.* **2024**, *22*, 7. [[CrossRef](#)] [[PubMed](#)]
63. Chiang, F.-F.; Huang, S.-C.; Yu, P.-T.; Chao, T.-H.; Huang, Y.-C. Oxidative Stress Induced by Chemotherapy: Evaluation of Glutathione and Its Related Antioxidant Enzyme Dynamics in Patients with Colorectal Cancer. *Nutrients* **2023**, *15*, 5104. [[CrossRef](#)] [[PubMed](#)]
64. Shim, H.S.; Bae, C.; Wang, J.; Lee, K.-H.; Hankerd, K.M.; Kim, H.K.; Chung, J.M.; La, J.-H. Peripheral and Central Oxidative Stress in Chemotherapy-Induced Neuropathic Pain. *Mol. Pain* **2019**, *15*, 1744806919840098. [[CrossRef](#)] [[PubMed](#)]
65. Jiang, H.; Zuo, J.; Li, B.; Chen, R.; Luo, K.; Xiang, X.; Lu, S.; Huang, C.; Liu, L.; Tang, J.; et al. Drug-Induced Oxidative Stress in Cancer Treatments: Angel or Devil? *Redox Biol.* **2023**, *63*, 102754. [[CrossRef](#)]
66. Luo, M.; Zhou, L.; Huang, Z.; Li, B.; Nice, E.C.; Xu, J.; Huang, C. Antioxidant Therapy in Cancer: Rationale and Progress. *Antioxidants* **2022**, *11*, 1128. [[CrossRef](#)]
67. Petrusheva, I.O.; Evdokimov, A.N.; Lavrik, O.I. Molecular Mechanism of Global Genome Nucleotide Excision Repair. *Acta Naturae* **2014**, *6*, 23–34. [[CrossRef](#)]
68. Holcomb, N.; Goswami, M.; Han, S.G.; Clark, S.; Orren, D.K.; Gairola, C.G.; Mellon, I. Exposure of Human Lung Cells to Tobacco Smoke Condensate Inhibits the Nucleotide Excision Repair Pathway. *PLoS ONE* **2016**, *11*, e0158858. [[CrossRef](#)]
69. Enjo-Barreiro, J.R.; Ruano-Ravina, A.; Pérez-Ríos, M.; Kelsey, K.; Varela-Lema, L.; Torres-Durán, M.; Parente-Lamelas, I.; Provencio-Pulla, M.; Vidal-García, I.; Piñeiro-Lamas, M.; et al. Radon, Tobacco Exposure and Non-Small Cell Lung Cancer Risk Related to BER and NER Genetic Polymorphisms. *Arch. Bronconeumol.* **2022**, *58*, 311–322. [[CrossRef](#)]
70. Wang, W.; Zhang, L.; Liu, L.; Zheng, Y.; Zhang, Y.; Yang, S.; Shi, R.; Wang, S. Chemosensitizing Effect of shRNA-Mediated ERCC1 Silencing on a Xuanwei Lung Adenocarcinoma Cell Line and Its Clinical Significance. *Oncol. Rep.* **2017**, *37*, 1989–1997. [[CrossRef](#)]
71. Fikrova, P.; Stetina, R.; Hrnčiarik, M.; Hrnčiarikova, D.; Hronek, M.; Zadák, Z. DNA Crosslinks, DNA Damage and Repair in Peripheral Blood Lymphocytes of Non-Small Cell Lung Cancer Patients Treated with Platinum Derivatives. *Oncol. Rep.* **2014**, *31*, 391–396. [[CrossRef](#)]
72. Lobachevsky, P.N.; Bucknell, N.W.; Mason, J.; Russo, D.; Yin, X.; Selbie, L.; Ball, D.L.; Kron, T.; Hofman, M.; Siva, S.; et al. Monitoring DNA Damage and Repair in Peripheral Blood Mononuclear Cells of Lung Cancer Radiotherapy Patients. *Cancers* **2020**, *12*, 2517. [[CrossRef](#)] [[PubMed](#)]
73. Sun, X.; Li, F.; Sun, N.; Shukui, Q.; Baoan, C.; Jifeng, F.; Lu, C.; Zuhong, L.; Hongyan, C.; YuanDong, C.; et al. Polymorphisms in XRCC1 and XPG and Response to Platinum-Based Chemotherapy in Advanced Non-Small Cell Lung Cancer Patients. *Lung Cancer* **2009**, *65*, 230–236. [[CrossRef](#)] [[PubMed](#)]
74. Zhou, C.; Ren, S.; Zhou, S.; Zhang, L.; Su, C.; Zhang, Z.; Deng, Q.; Zhang, J. Predictive Effects of ERCC1 and XRCC3 SNP on Efficacy of Platinum-Based Chemotherapy in Advanced NSCLC Patients. *Jpn. J. Clin. Oncol.* **2010**, *40*, 954–960. [[CrossRef](#)] [[PubMed](#)]
75. Liu, Z.; Liu, H.; Han, P.; Gao, F.; Dahlstrom, K.R.; Li, G.; Owzar, K.; Zevallos, J.P.; Sturgis, E.M.; Wei, Q. Apoptotic Capacity and Risk of Squamous Cell Carcinoma of the Head and Neck. *Eur. J. Cancer* **2017**, *72*, 166–176. [[CrossRef](#)] [[PubMed](#)]
76. Raturi, V.P.; Wu, C.; Mohammad, S.; Hojo, H.; Bei, Y.; Nakamura, M.; Okumura, M.; Rachi, T.; Singh, R.; Gupta, R.; et al. Could Excision Repair Cross-complementing Group-1 mRNA Expression from Peripheral Blood Lymphocytes Predict Locoregional Failure with Cisplatin Chemoradiation for Locally Advanced Laryngeal Cancer? *Asia-Pac. J. Clin. Oncol.* **2019**, *16*, e19–e26. [[CrossRef](#)]
77. Borgmann, K.; Röper, B.; El-Awady, R.A.; Brackrock, S.; Bigalke, M.; Dörk, T.; Alberti, W.; Dikomey, E.; Dahm-Daphi, J. Indicators of Late Normal Tissue Response after Radiotherapy for Head and Neck Cancer: Fibroblasts, Lymphocytes, Genetics, DNA Repair, and Chromosome Aberrations. *Radiother. Oncol.* **2002**, *64*, 141–152. [[CrossRef](#)]
78. Quintela-Fandino, M.; Hitt, R.; Medina, P.P.; Gamarra, S.; Manso, L.; Cortes-Funes, H.; Sanchez-Cespedes, M. DNA-Repair Gene Polymorphisms Predict Favorable Clinical Outcome Among Patients with Advanced Squamous Cell Carcinoma of the Head and Neck Treated with Cisplatin-Based Induction Chemotherapy. *JCO* **2006**, *24*, 4333–4339. [[CrossRef](#)]
79. Reed, E.; Yuspa, S.H.; Zwelling, L.A.; Ozols, R.F.; Poirier, M.C. Quantitation of Cis-Diamminedichloroplatinum 11 (Cisplatin)-DNA-Lntrastrand Adducts in Testicular and Ovarian Cancer Patients Receiving Cisplatin Chemotherapy. *J. Clin. Investig.* **1986**, *77*, 545–550. [[CrossRef](#)]
80. Stefanou, D.T.; Bamias, A.; Episkopou, H.; Kyrtopoulos, S.A.; Likka, M.; Kalampokas, T.; Photiou, S.; Gavalas, N.; Sfikakis, P.P.; Dimopoulos, M.A.; et al. Aberrant DNA Damage Response Pathways May Predict the Outcome of Platinum Chemotherapy in Ovarian Cancer. *PLoS ONE* **2015**, *10*, e0117654. [[CrossRef](#)]

81. Dimopoulos, M.A.; Souliotis, V.L.; Anagnostopoulos, A.; Bamia, C.; Pouli, A.; Baltadakis, I.; Terpos, E.; Kyrtopoulos, S.A.; Sfikakis, P.P. Melphalan-Induced DNA Damage in Vitro as a Predictor for Clinical Outcome in Multiple Myeloma. *Haematologica* **2007**, *92*, 1505–1512. [[CrossRef](#)]
82. Gkatzamanidou, M.; Sfikakis, P.P.; Kyrtopoulos, S.A.; Bamia, C.; Dimopoulos, M.A.; Souliotis, V.L. Chromatin Structure, Transcriptional Activity and DNA Repair Efficiency Affect the Outcome of Chemotherapy in Multiple Myeloma. *Br. J. Cancer* **2014**, *111*, 1293–1304. [[CrossRef](#)] [[PubMed](#)]
83. Gkatzamanidou, M.; Terpos, E.; Dimopoulos, M.A.; Souliotis, V.L. The Combination of Panobinostat and Melphalan for the Treatment of Patients with Multiple Myeloma. *Int. J. Mol. Sci.* **2022**, *23*, 15671. [[CrossRef](#)]
84. Stefanou, D.T.; Episkopou, H.; Kyrtopoulos, S.A.; Bamias, A.; Gkatzamanidou, M.; Bamia, C.; Liakou, C.; Bekyrou, M.; Sfikakis, P.P.; Dimopoulos, M.; et al. Development and Validation of a PCR-based Assay for the Selection of Patients More Likely to Benefit from Therapeutic Treatment with Alkylating Drugs. *Br. J. Clin. Pharmacol.* **2012**, *74*, 842–853. [[CrossRef](#)]
85. Autissier, P.; Soulas, C.; Burdo, T.H.; Williams, K.C. Evaluation of a 12-color Flow Cytometry Panel to Study Lymphocyte, Monocyte, and Dendritic Cell Subsets in Humans. *Cytom. Pt A* **2010**, *77A*, 410–419. [[CrossRef](#)] [[PubMed](#)]

Disclaimer/Publisher’s Note: The statements, opinions and data contained in all publications are solely those of the individual author(s) and contributor(s) and not of MDPI and/or the editor(s). MDPI and/or the editor(s) disclaim responsibility for any injury to people or property resulting from any ideas, methods, instructions or products referred to in the content.